Active health monitoring of an aircraft wing with an embedded piezoelectric sensor/actuator network: II. Wireless approaches

Smart Mater. Struct. **16** (2007) 1218–1225 doi:10.1088/0964-1726/16/4/033

Active health monitoring of an aircraft wing with an embedded piezoelectric sensor/actuator network: II. Wireless approaches

Xiaoliang Zhao[1,3], Tao Qian[1], Gang Mei[1], Chiman Kwan[1], Regan Zane[2], Christi Walsh[2], Thurein Paing[2] and Zoya Popovic[2]

[1] Intelligent Automation Inc., 15400 Calhoun Drive, Rockville, MD 20855, USA
[2] Department of Electrical and Computer Engineering, University of Colorado at Boulder, Boulder, CO 80309, USA

E-mail: xzhao@i-a-i.com

Received 24 October 2006, in final form 11 June 2007
Published 29 June 2007
Online at stacks.iop.org/SMS/16/1218

Abstract
The objective of this study is to develop a wireless ultrasonic structural health monitoring (SHM) system for aircraft wing inspection. In part I of the study (Zhao *et al* 2007 *Smart Mater. Struct.* **16** 1208–17), small, low cost and light weight piezoelectric (PZT) disc transducers were bonded to various parts of an aircraft wing for detection, localization and growth monitoring of defects. In this part, two approaches for wirelessly interrogating the sensor/actuator network were developed and tested. The first one utilizes a pair of reactive coupling monopoles to deliver 350 kHz RF tone-burst interrogation pulses directly to the PZT transducers for generating ultrasonic guided waves and to receive the response signals from the PZTs. It couples enough energy to and from the PZT transducers for the wing panel inspection, but the signal is quite noisy and the monopoles need to be in close proximity to each other for efficient coupling. In the second approach, a small local diagnostic device was developed that can be embedded into the wing and transmit the digital signals FM-modulated on a 915 MHz carrier. The device has an ultrasonic pulser that can generate 350 kHz, 70 V tone-burst signals, a multiplexed A/D board with a programmable gain amplifier for multi-channel data acquisition, a microprocessor for circuit control and data processing, and a wireless module for data transmission. Power to the electronics is delivered wirelessly at X-band with an antenna–rectifier (rectenna) array conformed to the aircraft body, eliminating the need for batteries and their replacement. It can effectively deliver at least 100 mW of DC power continuously from a transmitter at a range of 1 m. The wireless system was tested with the PZT sensor array on the wing panel and compared well with the wire connection case.

(Some figures in this article are in colour only in the electronic version)

1. Introduction

A significant number of civil and military aircraft have exceeded their design lifetimes: in 2000, 75% of US Air Force aircraft were more than 25 years old [2]. A major sustainment cost for these aging air vehicles is unscheduled maintenance. Structural health monitoring (SHM) technologies, by embedding smart sensors/actuators into the structures and responding/adapting to changes in condition, can help the transition from a schedule-based maintenance practice to condition-based maintenance

[3] Author to whom any correspondence should be addressed.

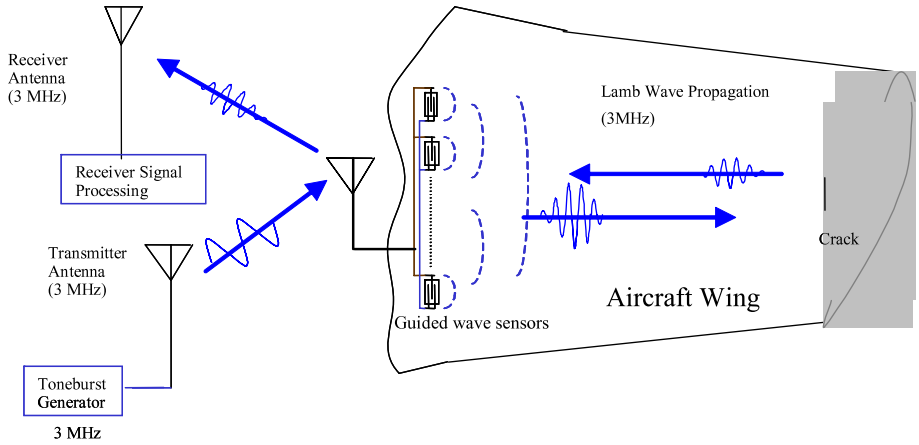

Figure 1. Schematic view of the direct analog RF coupling approach for aircraft wing inspection.

(CBM). The goal is to improve the maintenance agility and responsiveness for increased fleet availability, quicker turnaround time, and to reduce the total ownership cost over the life cycle [3]. As an example, inspection of a frequent structural problem or a defect-prone area (hot spot) at an inaccessible location requires a fast, low cost and reliable system for integrity monitoring to ensure the safety and functionality of the structure. One promising solution would be a SHM system that could be embedded into the structure, inspect the structural hot spots and download data or diagnostic results wirelessly to a remote station.

Existing work in wireless sensors for SHM applications includes inductively-coupled radio-frequency identification (RFID) temperature and electrochemical sensors that were developed to monitor the heat exposure of material underneath the thermal protection system (tiles) on the Space Shuttle, and the chloride ingress into concrete bridge decks, respectively [4]; a similar loop inductive coupling approach was used for pressure, humidity and chemical sensors [5]. Straser and Kiremidjian [6] proposed the integration of wireless communications with sensors based on a low-power 8-bit Motorola 68HC11 microcontroller. A good review article on wireless sensors for real-time health monitoring of civil structures is given in [7]. There are not many commercial available wireless sensor platforms at present. The Berkeley MICA Mote and MICA2 Mote are among the most popular platforms for implementing wireless sensor networks. For example, the MICA2 Mote was implemented in [8] and [9] for assessment of damage to building structures. A distributed SHM system based on MICA2 and a multi-agent technology for load and loose bolt monitoring on composites was developed in [10].

Most of the wireless SHM sensors that have been developed work at a low sampling rate, with low power requirement or in a passive mode [11]. Ultrasonic Lamb waves have recently been widely used for SHM applications by embedding PZT ceramic or wafer sensors in the structures. However, a wireless means of interfacing with those sensor/actuators is still not fully explored. There are two challenges for the development of a wireless ultrasonic SHM system: one is the high instantaneous voltage and power needed for exciting PZT actuators, and the other is the high sampling rate required for digitizing the ultrasonic signals. This paper extends our work on SHM of aircraft wings with embedded PZT transducer networks in part I [1] by introducing two wireless data acquisition approaches. In the first approach, a pair of electrically-short monopoles was used to deliver energy to the actuators and receive sensor signals through capacitive near-field coupling. It is easy to implement, and has been demonstrated to work well for PZTs both on a simple aluminum plate and on a real aircraft wing panel. However, this technique may not be practical for aircraft wing inspection if close access to the monopole transceiver on the aircraft is not granted. In addition, the noise level is relatively high for a direct analog signal coupling scheme. In the second approach, wireless sensors were integrated within the aircraft wing. A miniaturized diagnostic device with an on-board ultrasonic pulser, multiplexed A/D converter, microcontroller and a wireless module was embedded into the wing with the PZT sensor network. The device was also wirelessly powered with a microwave rectenna array, designed to conform to the aircraft wing and provide at least 15 V, 100 mW of DC power, from an 8 W, 10 GHz source at a range between 0.5 and 1 m. The wireless system was tested with the PZT sensor array on the wing panel, and it demonstrated comparable effectiveness for defect monitoring as with the wired system [1].

2. The direct RF capacitive coupling approach

A diagram of the technical approach is shown in figure 1. Ultrasonic guided wave transducer arrays are attached to wing structures such as a wing panel, with signal input/output connected to an on-board wire monopole. The interrogating RF tone-burst pulse is transmitted by a second wire monopole from a signal generator, received by the on-board monopole and converted to ultrasonic energy by the transducers. Guided waves in the frequency range between 100 kHz and a few megahertz are launched inside the structure, and scatter from defects or other discontinuities. The scattered waves are received by the transducers, converted back into electrical signals and coupled to a third receiving monopole. The monopoles are electrically short (about 58 cm long at 350 kHz) and made of aluminum tubes of diameter 6.5 mm. They are usually positioned in parallel and less than 10 cm apart

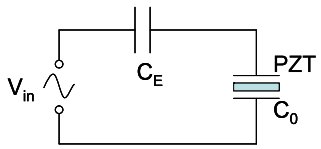

Figure 2. Equivalent circuit diagram of a pair of infinitesimal monopole antennae for coupling an RF signal directly to a PZT.

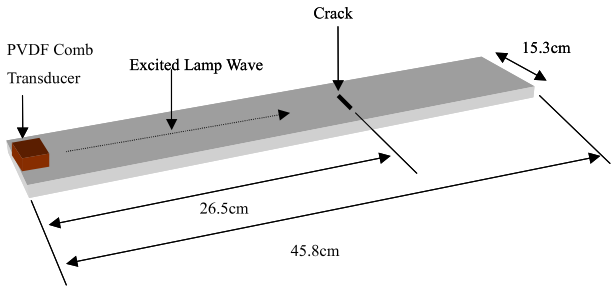

Figure 3. PVDF comb transducer bonded to the surface of the aluminum plate for crack inspection.

for efficient capacitive coupling [12], with an approximate equivalent circuit as shown in figure 2, where the monopoles are represented with the mutual capacitance C_E. Since the PZT transducers are capacitive in the megahertz frequency range, C_E should be as large as possible for efficient energy coupling via induced voltage. In this approach, both the transmitting and receiving monopoles can change positions when collecting inspection waveforms for the structure, in contrast to the conventional wired approach which, in general, uses bulky coaxial cables.

A simple proof-of-concept experiment with a machined notch simulating a defect in an aluminum plate is shown in figure 3. The plate is 0.8 mm thick, while the notch dimensions are 12 mm by 2 mm with depth 0.4 mm. Other relevant dimensions are shown in the figure. A polyvinylidene fluoride (PVDF) comb transducer which can generate an A_1 mode Lamb wave at 3 MHz [13] is mounted at one end of the plate and used to detect the simulated defect in a pulse-echo mode. The wireless test setup is shown in figure 4, where a transmitting short monopole is connected to an ultrasonic pulser for emitting RF energy; an on-board monopole antenna is connected to the PVDF transducer for receiving the RF energy that excites the PVDF transducer, and the defect echo signals are transmitted back to an active receiving monopole connected to a signal receiver/digitizer.

In the experiment, a Matec® TB-1000 tone-burst signal generator/receiver card was used to generate 3 MHz, 300 V peak-to-peak windowed sinusoidal pulses to the PVDF transducer through the transmission and onboard monopoles which are fabricated from aluminum tubes of diameter 6.5 mm. The feeding point is at the end of the tube. A Vectronics® active monopole and a Datel® PCI-417M2 40 megasamples per second (MSPS) digitizer were used for receiving and digitizing the return signal. Figure 5(a) shows the measured wireless signal waveform, and figure 5(b) shows the signal from a conventional wired inspection system for comparison.

The wireless echo signals from the notch and from the plate edge, respectively, are clearly seen on the screen with

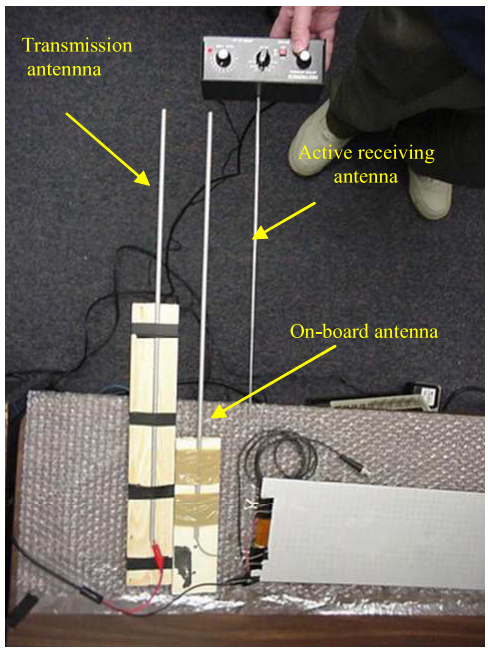

Figure 4. Wireless test setup. A transmitting monopole delivers RF pulses wirelessly through an on-board monopole to the PVDF transducer for generating Lamb waves, and another active monopole receives the ultrasonic echoes from the PVDF sensor through the same on-board monopole.

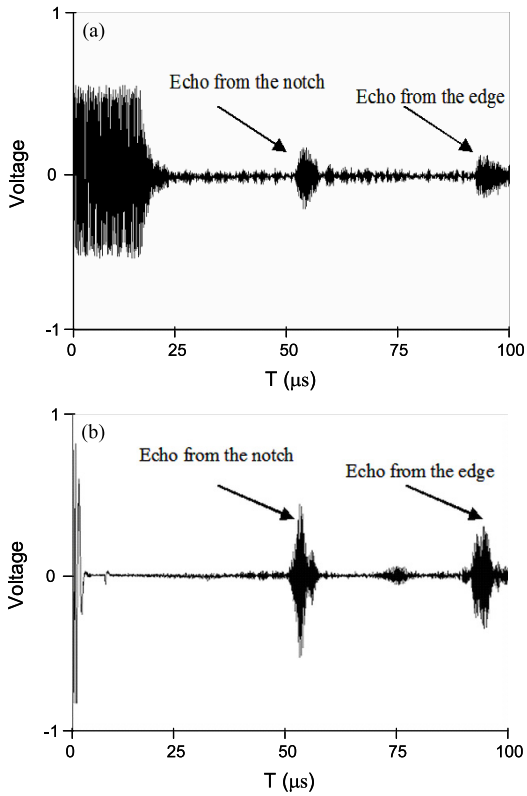

Figure 5. (a) Wireless and (b) wired inspection waveforms of the 12 mm long, 50% through wall notch in a 0.8 mm thick aluminum plate and 26.5 cm away from the PVDF transducer.

time domain averaging (25 times). However, the noise level is relatively high compared with the wired case. The long

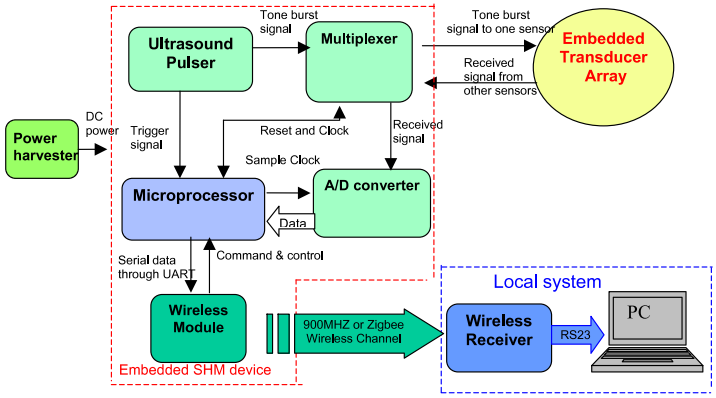

Figure 6. Diagram of the embedded ultrasonic structural health monitoring system.

main-bang is introduced by the active antenna, which may blind the defect signal if the defect is too close to the transducer. From this preliminary experiment, the direct wireless RF coupling concept proves to be feasible, although the monopoles need to be in close proximity (7–10 cm apart). We have also applied this approach to an aircraft wing panel, and similar signal conditions were observed. Defects such as rivet cracks and corrosion were successfully detected and located with an eight-sensor PZT array as in the wire connection approach in part I of the study [1]. Several directions have been pursued to improve the signal to noise ratio or to enhance the antenna efficiency; for example, a more powerful tone-burst generation source to increase the input energy, better sensor and monopole impedance matching, a more efficient antenna design, advanced signal processing algorithms for noise reduction, etc. However, the fundamental deficiency of the short coupling distance may still impede its application to aircraft wing SHM. We therefore pursued a microwave-frequency far-field wireless powering mechanism, described in the next section.

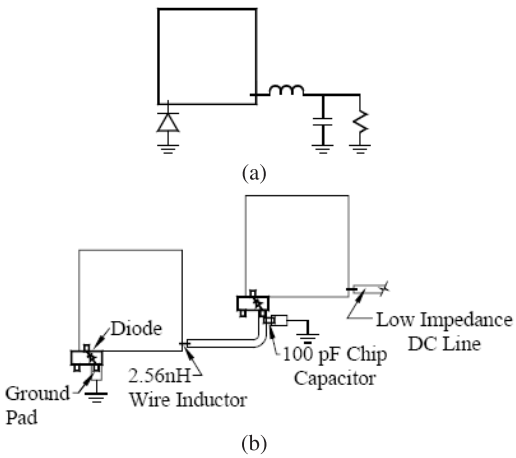

Figure 7. (a) Model for an ADS rectenna simulation circuit. The simulation uses a Spice model for the diode and models the antenna as an AC power source with a large series. The optimal lumped element values are determined to be $C = 100$ pF and $L = 2.56$ nH. (b) Layout of multiple elements connected in series.

3. Embedded local diagnosis approach

In the microwave-frequency wireless approach, a miniature ultrasonic diagnosis device was developed so that it can be embedded into structures with the transducer network for *in situ* data acquisition and processing. Figure 6 shows the system diagram. The embedded SHM device has an on-board tone-burst pulser that can generate 350 kHz, 70 V peak-to-peak tone-burst signals, a multiplexed A/D board with a programmable gain amplifier for multi-channel data acquisition, a low power consumption microprocessor for circuit control and data processing, and a wireless module for the download of data and processing results. On the ground or at a remote location, a wireless receiver and a computer console can receive the wireless data from the embedded SHM device and perform any necessary post-processing or display the results. The power for the embedded sensor system is provided wirelessly at 10 GHz from a transmitter and horn antenna at a 1 m range from the inspected aircraft wing. A conformal 10 GHz patch antenna array loaded with rectifiers (rectenna array) was designed to efficiently convert incident microwave power to DC power. When continuously illuminated with a power density of at most 10 mW cm^{-2}, it provides at least 100 mW of DC power with an open-circuit voltage of 15 V.

3.1. Rectenna array design

The design of the X-band rectenna array was presented in [14]. For the convenience of readers, some key features are repeated here. The rectenna element is a narrowband, linearly polarized patch antenna with a center frequency at 10 GHz designed on a 0.25 mm thick Rogers Duroid substrate with a permittivity of 2.2. The thin substrate allows the rectenna array to be flexible enough to conform to the moderate curvature of the airframe while desirable microwave properties are maintained. The antennas can be linearly polarized, since during monitoring of defects it is not difficult to co-polarize the rectenna and the transmitting powering antenna. For each rectifier/antenna element, an Agilent HSMS-8101 Schottky mixer diode was used. It was chosen based on its reported performance at 10 GHz and its availability. An ADS harmonic balance simulation using the model in figure 7(a) was used to optimize

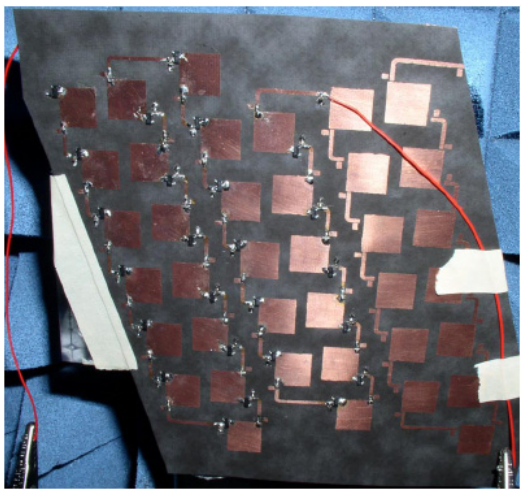

Figure 8. The 10 GHz 25-element microwave rectenna array for wireless powering of the on-board electronics. The antennas are narrowband patches made on a thin conformable substrate. Each antenna is loaded with a Schottky diode rectifier, and all elements are connected in series to enable the required 15 V output.

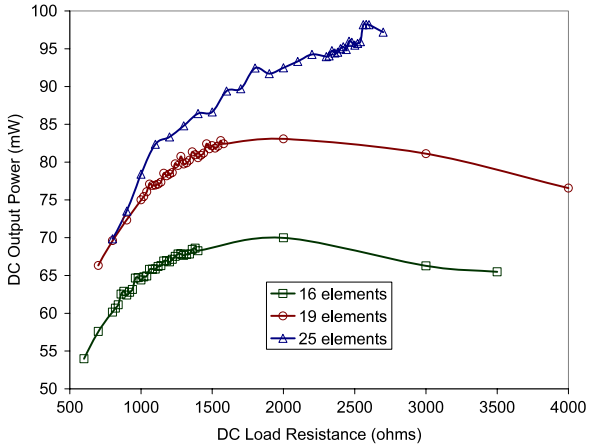

Figure 9. Measured output power as 9, 16 and 25 elements of the passive antenna array are populated with rectifier diodes, as a function of the DC load for a constant input power of 10 mW per element. The optimal load for the 25-element case is around 2.6 kΩ and results in the required 100 mW DC output power.

input and output impedances for maximum output voltage and power. The input impedance is found to be purely real. The maximum input impedance value is limited by the highest impedance of a manufactured patch antenna, around 200 Ω near the corner. The output circuit is an LC circuit, used as both the low pass filter and the matching circuit. The matching aspects of this circuit are more critical to the design for optimizing the output power [15]. The single element was simulated without considering connections to other rectenna elements. The maximum efficiency for the ideal circuit is 52% for an input power of 10 mW.

The total number of elements cannot be calculated directly from a single element because the efficiency of a rectenna array is lower than the efficiency of a single element [16]. Therefore, the minimum number of elements is calculated from the specified DC power and the efficiency of a single element. The minimum number of elements is calculated as

$$N = \frac{P_{\text{spec}}}{S_{\text{inc}} A_{\text{eff}} \eta}, \tag{1}$$

where N is the number of elements, P_{spec} is the specified DC power, S_{inc} is the incident power density, A_{eff} is the effective area of the antenna element and η is the rectification efficiency. Using a rectification efficiency of 50% and an effective area of 1 cm^2, a minimum of 20 elements will be required to provide 100 mW.

The rectenna array was fabricated using the layout in figure 7(b). A commercial lumped element capacitor and a small 0.24 mm diameter wire as the inductor provide the necessary impedance for the output filter. The relatively high voltage from the rectenna array with simple Schottky diode rectifiers is obtained by series connection of the antenna element DC outputs. This design is scalable: given an area available for the rectenna and the frequency of operation, the required transmitter power determines the power density and RF-to-DC conversion efficiency of the rectenna. Figure 8 shows a photograph of the rectenna array that was produced for the study, while figure 9 presents measured DC output power as a function of DC load impedance for three different array sizes, keeping the incident power density constant. It is seen that the optimal load impedance shifts as the number of series-combined voltage sources is increased. The rectenna conversion efficiency varies between 45% and 50% for different sized arrays.

In an ideal situation, an energy harvester will be able to collect ambient energy such as vibration or electromagnetic waves and convert them into electrical energy to power the embedded electronics and sensor array. Such a harvesting device for RF waves was demonstrated in [17] for broadband arbitrarily polarized incident microwave radiation.

3.2. On-board tone-burst pulser design and other electronics components

The rectenna designed in the previous section can provide enough power for the embedded electronics as well as the PZT transducers, but part of the DC output needs to be efficiently converted to 300–400 kHz windowed sinusoidal signals of at least 70 V peak-to-peak to excite the PZTs. Figure 10(a) shows a circuit design schematic for a tone-burst pulser that does the work, and figure 10(b) shows the produced circuit board for the SHM system. The converter design is based on a half-bridge series resonant inverter with an isolated output. It can generate 70 V peak-to-peak tone-burst pulses every 10 ms, with the center frequency tunable from 300 to 400 kHz. Care was taken to select timing circuitry with very low standby current and fast start-up to meet the timing and limited power budget requirements. The design uses two timers: a low power, low frequency (TLC555) timer for the 10 ms pulse period and a high frequency (LTC6906) timer for pulsed converter operation. Additional circuitry is used to achieve fast dissipation of resonant energy and fast output shutdown at the end of each burst. The resonant frequency was chosen near the operating frequency as a compromise between circulating current losses and sensitivity to variations in the effective load capacitance. The total power consumption of the pulser is less

Table 1. Comparison of U-MOTE with existing MICA2 and WISP wireless sensor platforms.

	U-MOTE	MICA2	WISP
MCU	MCU C8051F120	ATMegal128L	ATK94K10L/40L
ADC	ADC1173, 8 bits	Internal, 10 bits	AD9200, 10 bits
Sampling rate	10 MSPS (up to 15 MSPS)	Up to 16 kSPS	10 MSPS (up to 20 MSPS)
Memory	Internal RAM (8 kB + 256) + 128 kB flash	SRAM (24 kB) + flash	External SRAM (256 k × 16 bits)
Ultrasound pulser	300–400 kHz tone burst, 70 Vp-p	(none)	(none)
Mux–demux	8 × 8 channels (up to 16 × 16), 200 Vp-p	4 channel input, 3 Vp-p	(none)
Power consumption estimation[a] (mW)	30(MCU) + 33(ADC) + 30 (pulser) + 60(mux–demux) + 30(RF Tx) + 20(RF Rx)	17(MCU) + 80(RF Tx) + 30 RF(RF Rx)	24(MCU) + 60/120(FPGA) + 126(RF Tx) + 87(RF Rx)

[a] based on 3 V DC input.

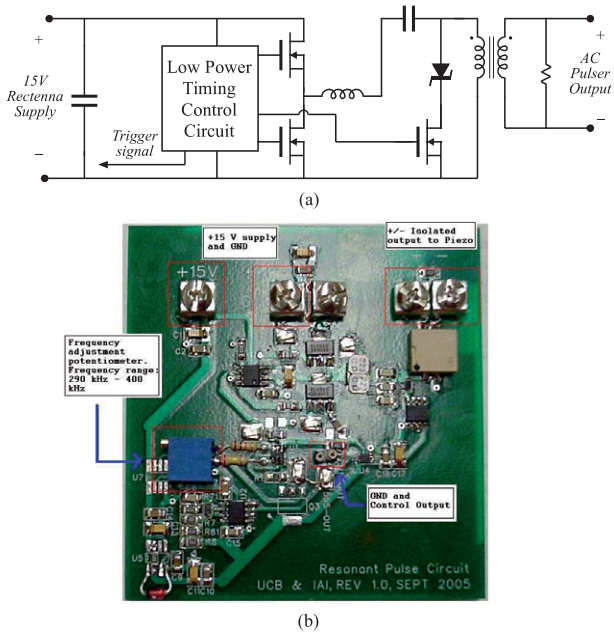

Figure 10. Ultrasound tone-burst pulser: (a) simplified schematic and (b) printed circuit board for the structural health monitoring system. The complete pulser circuit consumes less than 30 mW at 0.2% duty cycle and 70 V peak-to-peak output.

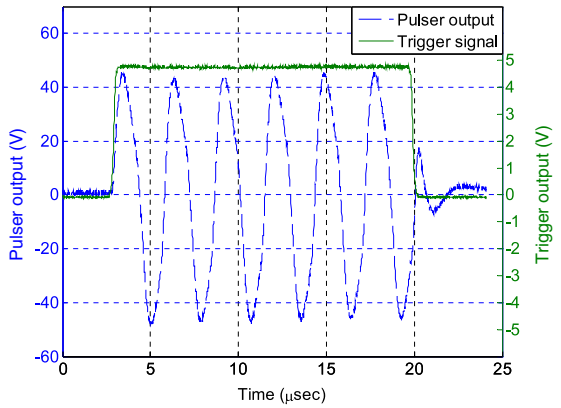

Figure 11. Tone-burst output from the on-board pulser. Trace (1) shows the pulser output voltage (dashed line, left scale), and (2) shows the control signal output (solid line, right scale).

than 30 mW for 0.2% duty cycle operation. Figure 11 shows a typical tone-burst signal and the trigger signal from the pulser, where the low duty cycle results in seven or eight cycles of sinusoidal output per burst.

In order to interface with the transducer network on board, a multiplexer and de-multiplexer (mux–demux) is needed to interrogate each pair of actuator/sensor elements. The mux–demux developed in this paper currently has 8 × 8 channel capability, but is expandable to 16 × 16 channels or more. It is made of low-power-consumption mechanical relays to eliminate crosstalk problems found in solid state or laser diode switches. A drawback of the mechanical relay is the relatively high power consumption (∼30 mW) and slow response time (around 1 ms for switching on/off). This is still tolerable in this work since channel switching is not frequent for pair-wise PZT data collection. The mux–demux can pass 200 V peak-to-peak ultrasonic signals and finish a round of data collection for an eight-element sensor array within a minute. The A/D converter has 8-bit resolution and a sampling rate of 10 MSPS sampling rate. It also has a programmable-gain amplifier so that signals from different channels can be compensated to the same amplitude level for fully utilizing the digitization resolution. The wireless modules used for data transfer from the SHM device to a local PC are LINX ES Series RF modules. Firmware communication protocol was developed to handle packet generation, processing, synchronization, and error detection and correction. All the electronics boards, including the tone-burst pulser, the multiplexer, A/D converter, microprocessor, and the wireless module, were put into a metal box of 6.75 inch × 4.75 inch × 2 inch in dimension (see figure 12). It could be further miniaturized with careful circuit layout and board integration.

Table 1 summarizes the key features of this ultrasonic wireless diagnosis device (U-MOTE) compared with some existing wireless sensor platforms, e.g. MICA2 and WISP [11]. The most noticeable feature of our platform is the on-board 70 V tone-burst pulser and the high voltage mux–demux designed for multi-channel ultrasonic data acquisition. To the authors' best knowledge, these features are not yet available in existing platforms. Note that the power consumption of this device is relatively high compared with MICA2 during operation. A rechargeable battery supplemented with a power

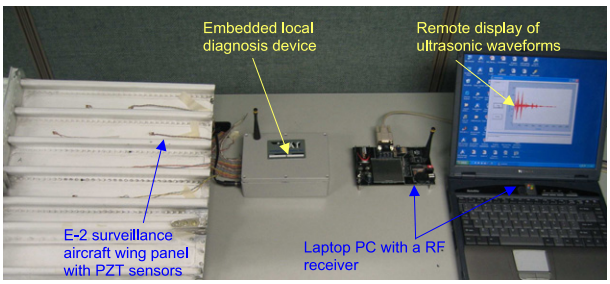

Figure 12. Embedded ultrasonic data acquisition and wireless transfer system for an E-2 wing panel inspection.

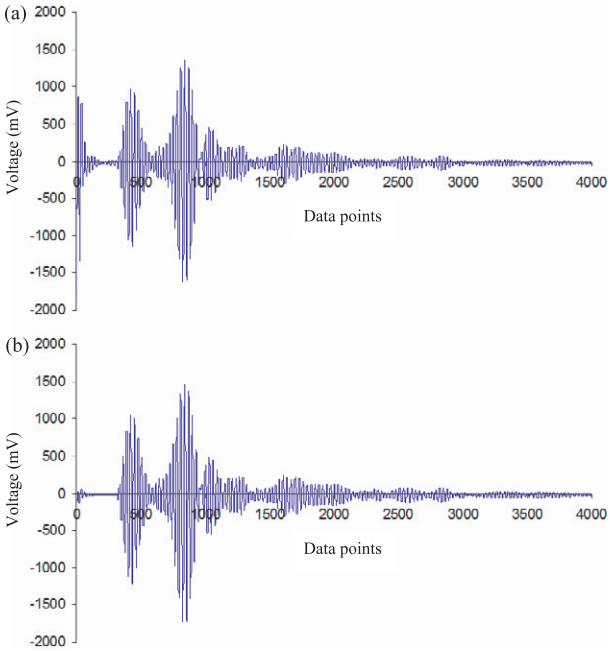

Figure 13. Comparison of ultrasonic guided wave data collected by (a) the wireless SHM device and (b) the direct wire connected instrument.

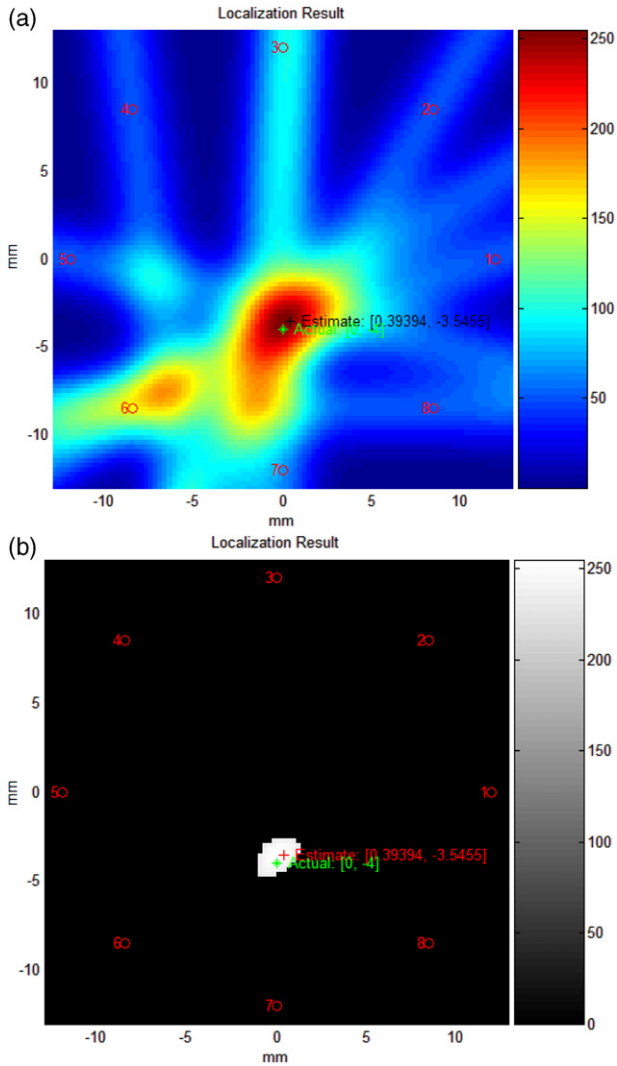

Figure 14. Defect detection and location estimation with the embedded wireless ultrasonic data acquisition system and the RAPID algorithm [1]: (a) the defect probability density map for the loose rivet; (b) estimating the defect location by setting a threshold to the probability density map.

harvesting unit seems to be a viable way to power the device for a short period of time of active defect monitoring; and while in the sleep mode, the battery could be recharged.

3.3. Performance test on an aircraft wing panel

The test setup for an aircraft wing panel inspection is shown in figure 12. As in part I of the study [1], an eight-element 350 kHz PZT transducer array was installed on the inner surface of the E-2 wing panel. The transducer input/output was connected to the embedded SHM diagnosis device that can generate a tone-burst signal and collect sensor data. With the LINX RF module, the collected ultrasonic guided wave data were successfully transferred from the on-board SHM device to a PC processing station 2–3 m away. Close-to-real-time data collection and display were achieved with the 36.8k baud rate LINX RF link. Figure 13 shows two waveforms collected on the wing panel with the same PZT transducers by the wireless embedded device, and by a direct wire connection, respectively. It is seen that the wireless waveform agrees quite well with the direct wire connection signal except at the very beginning where electromagnetic coupling effect is stronger than the wire connection case.

Similarly, we drilled a rivet out of the E-2 wing panel within the PZT transducer ring array and used the wireless SHM system to collect pair-wise PZT ultrasonic guided wave data for defect detection and localization. The data collected were transferred wirelessly to a laptop PC and processed with the RAPID algorithm developed in part I [1]. Figure 14(a) shows the defect distribution probability map and (b) its estimated location after applying a proper threshold to figure 14(a). The estimated defect location agrees very well with the true location. This test proves the feasibility of using the embedded PZT transducer network and diagnosis device for wireless *in situ* structural integrity monitoring of aircraft wings.

4. Conclusions

Two wireless ultrasonic SHM approaches have been realized in this study. The first approach, i.e. the direct RF analog signal coupling approach, requires only passive transducers and an antenna to be embedded inside the structure while the energy is coupled to the transducer with an external transmitting antenna. Due to the reactive coupling nature, the transmitting and receiving devices have to be in close proximity. While this approach may not be practical for remote integrity monitoring of an aircraft, it could be a wireless solution for applications when distance is not an issue. The second approach embeds both the transducer network and the data acquisition device into a structure, while the data can be downloaded wirelessly through a radio with good signal quality, range, and immunity to interference. Power is delivered wirelessly to the module at X-band with a rectenna array conformed to the aircraft body, eliminating the need for batteries or battery replacement. The demonstrated system delivers at least 100 mW of DC power continuously from a transmitter at a 1 m range. Experimental results were demonstrated for a fully embedded system with a PZT sensor array on the wing panel, including accurate defect detection and location estimation.

Acknowledgments

This work was partially supported by US Naval Air Systems Command under SBIR contract N68335-02-C-3105. The authors would also like to thank Dr Vinod Agarwala and James Stephenson of NAVAIR for providing the wing specimens and helpful discussions.

References

[1] Zhao X *et al* 2007 Active health monitoring of an aircraft wing with embedded piezoelectric sensor/actuator network: I. Defect detection, localization and growth monitoring *Smart Mater. Struct.* **16** 1208–17

[2] Staszewski W J, Boller C and Tomlinson G R 2004 *Health Monitoring of Aerospace Structures* (West Sussex: Wiley)

[3] Derriso M M and Olson S E 2005 The future role of structural health monitoring for air vehicle applications *Proc. 5th IWSHM* ed F K Chang, pp 17–25

[4] Watters D G *et al* 2002 Design and performance of wireless sensors for structural health monitoring *Rev. QNDE* **21** 969–76

[5] Ong K G and Grimes C A 2000 A resonant printed-circuit sensor for remote query monitoring of environmental parameters *Smart Mater. Struct.* **9** 421–8

[6] Straser E G and Kiremidjian A S 1998 A modular, wireless damage monitoring system for structures *Technical Report 128* John A Blume Earthquake Engineering Center, Stanford University, Stanford, CA

[7] Lynch J P and Loh K 2005 A summary review of wireless sensors and sensor networks for structural health monitoring *Shock Vib. Dig.* **38** 91–128

[8] Chintalapudi K *et al* 2005 Structural damage detection and localization using wireless sensors networks with low power consumption *Proc. 5th IWSHM* ed F K Chang, pp 1251–8

[9] Nitta Y *et al* 2005 Rapid damage assessment for the structures utilizing smart sensor MICA2 MOTE *Proc. 5th IWSHM* ed F K Chang, pp 283–90

[10] Yuan S *et al* 2006 Distributed structural health monitoring system based on smart wireless sensor and multi-agent technology *Smart Mater. Struct.* **15** 1–8

[11] Liu L and Yuan F G 2005 Design of wireless sensor for high frequency applications *Proc. 5th IWSHM* ed F K Chang, pp 1602–9

[12] Balanis C A 1997 *Antenna Theory* (New York: Wiley)

[13] Zhao X, Kwan C and Luk K M 2004 Wireless health monitoring of an aircraft wing *Proc. 16th WCNDT (Montreal, Canada)*

[14] Walsh C, Rondineu S, Jankovic M, Zhao X and Popovic Z 2005 A conformal 10 GHz rectenna for wireless powering of piezoelectric sensor electronics *Microwave Symp. Digest* (Long Beach, CA: IEEE MTT-S IMS)

[15] Hagerty J 2003 Nonlinear circuits and antennas for microwave energy conversion *PhD Thesis* University of Colorado at Boulder

[16] Gutmann R and Borrego J M 1979 Power combining in an array of microwave power rectifiers *IEEE Trans. Microw. Theory Tech.* **27** 958–68

[17] Hagerty J A, Helmbrecht F B, McCalpinW H, Zane R and Popovic Z 2004 Recycling ambient microwave energy with broad-band rectenna arrays *IEEE Trans. Microw. Theory Tech.* **52** 1014–24